Dynamic Analysis of the Santana do Cartaxo Viaduct: Definition of the Experimental Verification using Statistical Analysis of the Numerical Results

A.H. Jesus, Z. Dimitrovová and M.A.G. Silva

Department of Civil Engineering, Faculdade de Ciências e Tecnologia Universidade Nova de Lisboa, Caparica, Portugal

In J. Pombo, (Editor), "Proceedings of the First International Conference on Railway Technology: Research, Development and Maintenance", Civil-Comp Press, Stirlingshire, UK, paper 5, 2012. doi:10.4203/ccp.98.5

Abstract

The dynamic behaviour of a railways viaduct modelled after an actual structure located in Santana do Cartaxo, Portugal, is analysed through a parametric statistical analysis. Most previous work on parametric analyses of railway bridges considered the influence of key parameters individually, leading sometimes to contradictory conclusions. Simultaneous consideration of the influence of several key parameters provides a better representation of reality associated with the application of statistical analysis. In this study the key parameters selected are the train speed and some of the parameters known to contribute to ballast behaviour. Natural frequencies, maxima in displacements and accelerations at mid-point of bridge spans were chosen as key response measures. The load applied corresponds to the locomotive used in the Intercidades train. In the preliminary stages, either one axle load is applied, or two axle loads moving in opposite directions are introduced. Factorial experimentation was selected for the statistical analysis. The viaduct model was developed using the ANSYS/LS-DYNA module. Results are shown and interpreted.

Keywords: dynamic analysis, railway bridges, key input data, key results, statistical analysis, design of experiments.

1 Introduction

Dynamic analyses of railway bridges are still subject of research given some uncertainties both on material characterization and on the numerical procedures associated to the model selected to represent the system. For instance, rules and strategies for execution of numerical analyses are not yet well-defined and levels of possible simplifications and computational guidelines are not uniformly established.
Simplified models of railway tracks are widely used when nonlinear effects like, *e.g.*, irreversible ballast settlements have to be taken into account. However if such

nonlinearities are important to the response sought, complete models involving all structural details are preferable. The application of the finite element method (FEM) to model computationally the system requires careful choices (i) types of elements; (ii) size of model; (iii) size of the finite elements; and (iv) treatment of boundary conditions.

Design engineers often completely rely on the output originated from the FE calculations and seldom check or verify the accuracy of the results obtained. Railway bridges, in turn, are complex structures that require simplifications and imply uncertainties always present in the numerical analysis of their dynamic behaviour. Actually, the potential of statistical methods analysis to mitigate some of those limitations is often overlooked and seldom used among structural engineers.

Another very important aspect to consider when a numerical model of a complex structure like a railway bridge or a viaduct is developed for running dynamic analyses, is the posterior calibration of input data by experimental verification. In-situ measurements are quite expensive and therefore what to measure and where to do it must be carefully studied. A numerical analysis can help to optimize such a preparation.

By statistical analysis of numerical results obtained it is possible to establish a set of key input data and key results. Key input data in this context are defined as the ones whose change causes the largest changes in key results. Traditionally only one input parameter influence was analysed at each stage. Recently, the importance of studying the joint effect of several modelling parameters has been proven.

Satisfactory statistical analyses have to be supported on numerical models computationally accessible that provide results with sufficient accuracy. When statistical analysis is concluded, then the key results determined represent the characteristics to be measured by in-situ experiments. The key input data serve a twofold objective: (i) they are used for model calibration, (ii) they dictate additional tests to be performed in laboratory environment, in order to provide better estimates of the value to be implemented in the numerical model.

The work presented in the sequel was performed as part of project SMARTRACK dedicated to research on the area of integrated response of trains, railways and supporting structures. One of the case studies selected by the industrial partner of the project, REFER EP, was a segment of track involving the Santana do Cartaxo viaduct, located in Portugal and a database from REFER was used for definition of the relevant data. The numerical model was developed in an ANSYS/LS-DYNA module. The parametric analyses with automatic extraction of key results are coded by APDL (ANSYS parametric design language) [1]. Several structural simplifications were introduced: (i) railpads and ballast are represented by spring and damper elements; (ii) rails, sleepers, pillars, foundation block and piles are approached by beam elements; (iii) shell elements are used for viaduct tray; (iv) only a part of soil layers is modelled by 3D elements. Waves reflection is prevented by damping elements defined by Lysmer´s absorbing boundary condition [2], soil layer until the rock foundation is substituted by representative springs [3]. At this bottom surface Lysmer dampers are also included.

The paper is organized in the following way: in Section 2 the case study is described. In Section 3 FE model and its variants are defined. In Section 4 several

result comparisons are performed. In Section 5 preliminary results of parametric and statistical analyses are shown and the paper is concluded in Section 6.

2 Case study

2.1 General description

Necessary information regarding the structure, train specification and in-situ measurements was supplied by the industrial partner of the SMARTRACK Project, REFER EP. The case study is inserted in the Portugal North Line, second sub-link Setil Sul Vale de Santarém, which develops from km 56+625 until km 65+287. The rehabilitation of the North Line follows closely the original design, except for the Santana do Cartaxo segment where a new railway is included, over a viaduct built at km 59+000 to km 60+000 (Figure 1).

Figure 1: Santana do Cartaxo viaduct.

The viaduct is developed lengthwise by a set of eight module sections. Each module is connected to the other through transition pillars which are larger and have more piles than the intermediate pillars. The spans that connect with the transition pillars were enlarged by 3m to make up for the expansion joints of 6m. Each module has always the same intermediate pillars, that support the deck and connect to the

foundation. There are 46 pillars with a height around 7m. They rest on a concrete block that is connected with two piles. The piles have a diameter of 1.5m and can reach a depth of 30 to 35m.

One of the eight sections has three spans of 25, 30, and 25m, giving a total length of 80m, while the other seven modules have spans of 25, 4x30 and 25m, yielding the total length of 170m, bringing the total viaduct length to 1312m. The viaduct assents at its ends on two embankments that are modelled through additional modules supported by representative springs at the end of the viaduct. The length of these additional modules is 30m each.

On the plan view (see Figure 2) the viaduct develops linearly and at the end starts a left transition curve of the final radius 1750m. For the sake of simplicity the FEM model was developed for a fully straight line.

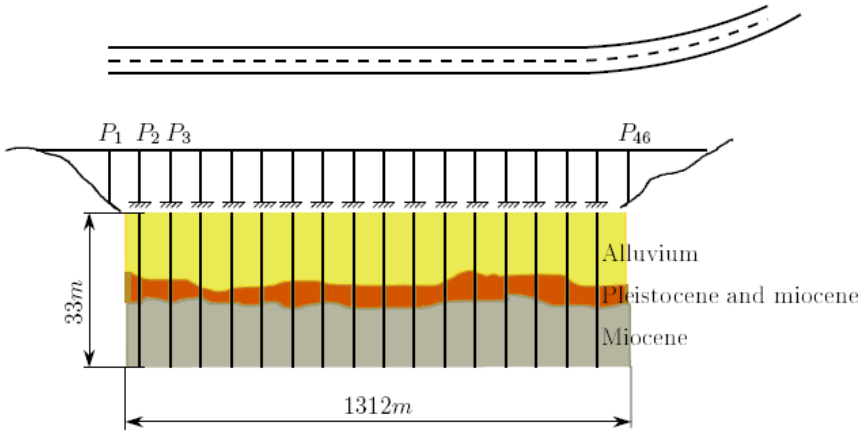

Figure 2: Viaduct top and left view showing the soil geological composition.

Geotechnical unit	γ [kN/m^3]	G [MPa]			ν	E [MPa]	
		γ=10^{-6} (G_0)	γ=10^{-4}	γ=10^{-3}		γ=10^{-4}	γ=10^{-3}
Clay and sits (“A1”)	16	19.8	19.8	10.9	0.49	59	32.5
Fine sand and siltose clays (“A2” and “A3”)	18	36	28.8	14.4	0.35	77.7	38.9
Over-consolidated clays (“P-M”)	20	66.1	59.5	36.4	0.48	176.1	107.7
Miocene (“M”)	21.5	350	298	157	0.25	745	392.5

Table 1: The relevant geological data.

According to the geological prospecting data the stratigraphy classification (Figure 2) revealed the presence of:

- Alluvium (14m)
- Pleistocene and Miocene (5m)
- Miocene

This last substratum can be characterized as an effectively stiff soil and was therefore chosen as an appropriate base for the foundations. 3m were still modelled, meaning that the structure is represented until 22m below the soil surface.

The relevant geological data for each substratum (soil constants) are given in Table 1, where γ, E, G and ν stand for volumetric weight, Young´s modulus, shear modulus and Poisson´s ratio, respectively. Alluvium layer is classified into three groups, designated A1, A2 and A3. P-M and M stand for the Pleistocene and Miocene and Miocene, respectively.

2.2 Load

Figure 3: Alfa Pendular train.

Figure 4: Intercidades train.

The traffic over the viaduct is practically equally distributed between Alfa Pendular (Figure 3) and Intercidades trains (Figure 4), travelling at maximum speed of 220km/h. There also passes the Regional train, but this one traverses the viaduct at lower velocity, with maximum speed established as 190km/h. The load applied corresponds to Intercidades locomotive. In preliminary studies either one axle load is applied, or two axle loads passing in opposite directions are implemented. The axle load of 213kN is rounded to 200kN, giving a force equal to 100kN applied at each rail. Reference velocity was selected as 50m/s=180km/h.

3 Finite element model

3.1 Element types

Three dimensional FE model is created in the explicit dynamic module LS-DYNA of ANSYS. In order to run statistical and parametric analyses, the finite element model must be computationally accessible. This is the reason why explicit non-linear dynamics solver was chosen. Solutions can be obtained faster than by implicit solvers, but the disadvantage is that the model can become unstable more easily. In order to reduce the computational time even more, several simplifications were implemented especially on the superstructure level. On the other hand, foundation conditions were considered important and therefore a part of the soil surrounding pillars was included in the model. Because LS-DYNA module does not have modal analysis, equivalent FE model was also created in ANSYS regular module. Unfortunately this was not a straightforward task, due to different element types used and different introduction and arrangement of element characteristics.

The main SMARTRACK project requirement demanded analyses involving all important structural non-linearities, especially on ballast, and that slowed down the analysis. Therefore several models with different simplifications were tested. Regarding the non-linearities mentioned above, linear and cubic response according to [4] were considered at the ballast level; linear and non-linear behavior according to [5] at the railpads level.

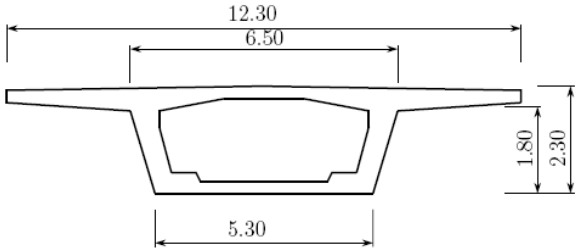

Figure 5: Viaduct tray cross-section.

Several simplifications that keep the computational effort at a tractable level are implemented. Railpads and ballast are represented by linear and rotational spring and damper elements acting in three directions, in the same way as reported in [6].

Rails, sleepers, pillars, foundation block and piles are approached by beam elements. The viaduct pillars are modelled with a rectangular section and are connected at the top to the shell elements that represents the lower deck. The connection allows for rotation in the longitudinal direction. The viaduct piles and foundation block are idealized as a pair of beams connected by a third a concrete block. Beam elements are superposed directly on the edges of soil elements to avoid additional constraints. Shell elements are used for the viaduct tray (see Figure 5).

Foundation soils were considered until the 3m of Miocene substratum as mentioned in Section 2.1. giving the active depth of H=22m. Nevertheless, only 6m deep soil layer is modelled by 3D elements. The "missing" layer of 16m depth, i.e. till the depth where rigid constraints are assumed, is substituted by representative springs [3] of the following stiffnesses in the normal and tangential directions, k_n and k_t, respectively:

$$k_n = \frac{\lambda + 2\mu}{H - h} = \frac{E(1-\nu)}{(1+\nu)(1-2\nu)(H-h)} = \frac{E^{oed}}{(H-h)} \tag{1}$$

$$k_t = \frac{\mu}{H - h} = \frac{E}{2(1+\nu)(H-h)} = \frac{G}{(H-h)}, \tag{2}$$

where λ, μ, E, E^{oed}, G and v are the two Lame´s constants, Young´s modulus, oedometer modulus, shear modulus and Poisson´s ratio of the replaced soil. H is the active depth and h the depth of the soil in the model. Due to the presence of different soil layers within H-h, equivalent springs were used.

This dynamic analysis in principle involves soils of infinite dimensions represented by a finite model. Therefore special transmitting, absorbing or non-reflecting boundaries were introduced on the artificial model boundaries. A number of these were proposed in the past with recourse to various mathematical or physical principles, but all of them are mathematically equivalent, and must have comparable wave-absorbing attributes [7]. Unfortunately, none of the transmitting boundaries can fully prevent all possible reflections under the full range of possible incident angles. The better the performance of the absorbing boundary, the smaller the model that can be used. Lysmer's boundary according to [2] was checked and implemented in the FE model introducing the following viscous damping coefficient in normal, c_n, and tangential, c_t, directions:

$$c_n = \rho v_p, \; c_t = \rho v_s, \tag{3}$$

where ρ is the soil density and v_p and v_s are velocities of propagation of pressure (primary) and shear (secondary) waves. These dampers absorb effectively pressure and shear waves, which does not apply to Rayleigh superficial waves. Nevertheless, in previous work we found Lysmer's damper performance satisfactory even at the soil surface, when introduced at a reasonable distance from the source.

Despite LS-DYNA capability of direct definition of non-reflecting boundaries, for better control and possible adaptation, it was decided to create the boundary "manually". As for the representative springs, values in Equation (3) are distributed,

and therefore for discrete dampers they must be multiplied by the area of influence, see Figure 6.

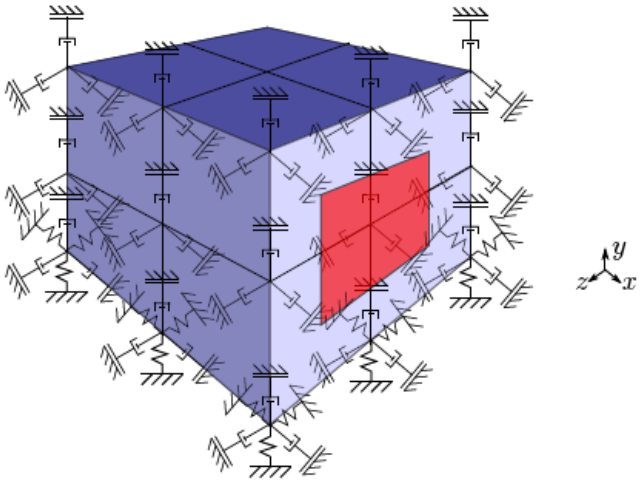

Figure 6: Spring and damper elements at soil surfaces, influence area definition.

In Figure 6 the area of influence is designated by red colour, and in solid elements corresponds to the sum of the four quarters of the adjacent elements faces. Figure 6 shows that the area of influence at the soil borders and corners in the regular mesh reduced by half or quarter, respectively. This difference was omitted in the model.

Next Figures 7-8 show different views of the first modulus without embankment.

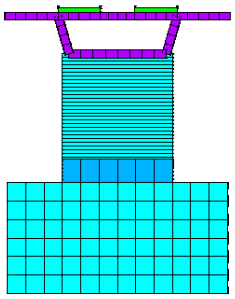

Figure 7: Frontal view – first modulus.

3.2 Spring/damper system of ballast and railpad modulation

The spring/damper system to model ballast and the implemented finite element structure is as used in [6]. A scheme of the system is displayed in Figure 9 (later in the text). The ballast and railpads are idealized as a set of linear and rotational Maxwell systems coupled together. The linear springs and dampers act in the three directions; rotational springs and dampers are introduced only in longitudinal and lateral directions. This representation is introduced separately for the ballast (two

systems under each sleeper) and for each railpad. Ballast mass is inserted as two mass elements, m_b. Distance between these systems in longitudinal direction is 0.6m.

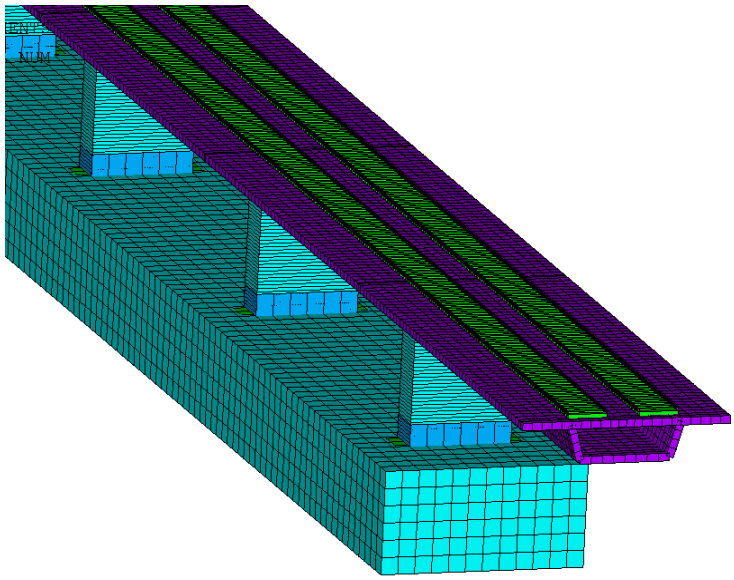

Figure 8: Perspective view – first modulus.

Material data are summarized in Table 2 (later in the text).

3.3 Other materials

The viaduct is exclusively made from pre-stressed concrete, the deck and piles (C4555) being more resistant than the pillars and foundation block (C3037). Material data are summarized in Table 4. PSC stands for pre-stressed concrete used in sleepers. Input data related to UIC60 rail are summarized in Table 4.

Material	E (GPa)	v	ρ (ton/m^3)
C3037	33	0.3	2.5
C4555	36	0.3	2.5
PSC	30	0.2	2.054

Table 3: Material data.

Property	Beam (2 UIC60)
Young's modulus E (GPa)	210
Poisson's ratio v	0.3
Density ρ (kg/m^3)	7800
Cross-section area A (m^2)	$76.84 \cdot 10^{-4}$
Moment of inertia I (m^4)	$3055 \cdot 10^{-8}$

Table 4: UIC60 rail data.

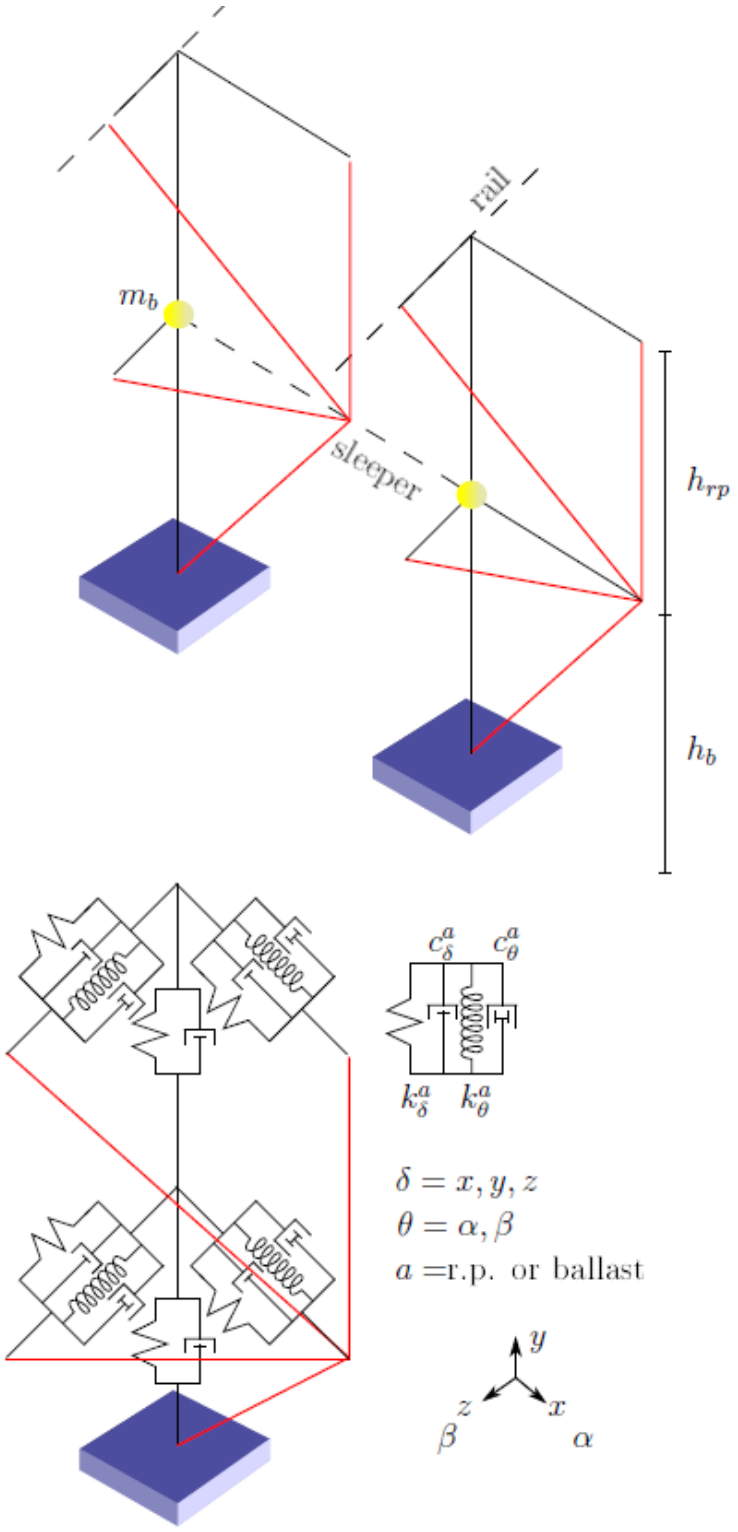

Figure 9: Spring/damper system of ballast and railpad modulation, red lines represent the connectors to the massless points.

Parameter	Value
h_{rp}	0.196m
h_b	0.30m
m_b	1.3225ton
k_y - ballast	120000kN/m
c_y - ballast	70kNs/m
k_x - ballast	40000kN/m
c_x - ballast	52kNs/m
k_z - ballast	40000kN/m
c_z - ballast	52kNs/m
k_α - ballast	676kNm
c_α - ballast	394kNs
k_β - ballast	676kNm
c_β - ballast	394kNs
k_y – rail pad	280000kN/m
c_y – rail pad	50kNs/m
k_x – rail pad	50000kN/m
c_x – rail pad	10kNs/m
k_z – rail pad	50000kN/m
c_z – rail pad	10kNs/m
k_α - rail pad	597kNm
c_α - rail pad	0.107kNs
k_β - rail pad	597kNm
c_β - rail pad	0.107kNs

Table 2: Material data of the spring/damper system of ballast and railpad modulation.

4 Comparative results

First comparative results evaluated the effect of single versus opposing axle loads, moving at the constant reference velocity of 180km/h. Deformed shape (in m) is shown for these two cases in Figures 10-11. The second load is advanced in order to evaluate the torsional resistance of the viaduct. Therefore when the second load is already in the middle of the structure, the first load is still only in the middle of the first span.

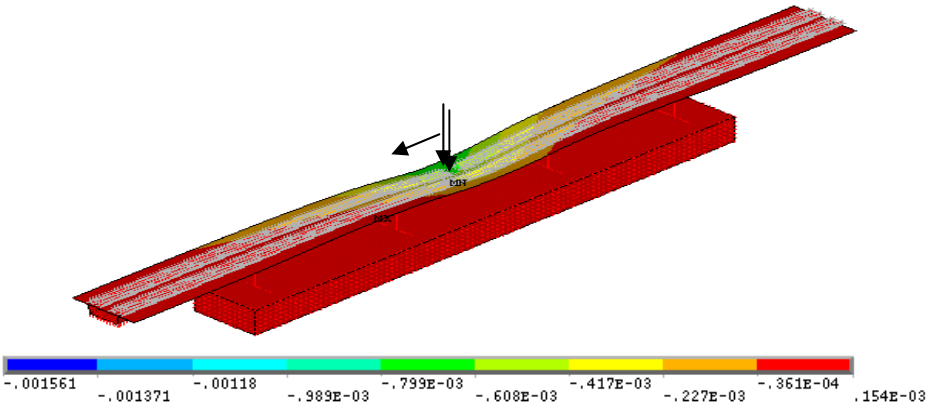

Figure 10: Deformed shape of the first modulus subjected to one axle load.

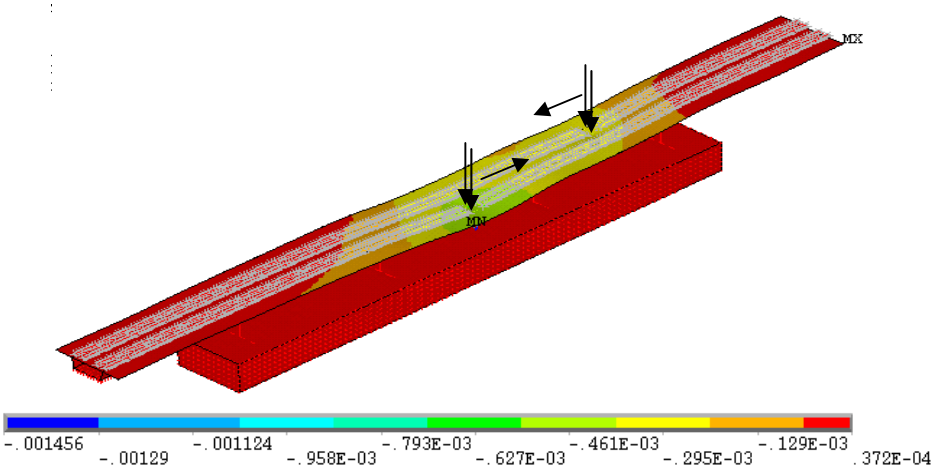

Figure 11: Deformed shape of the first modulus subjected to two axle loads moving in opposing directions.

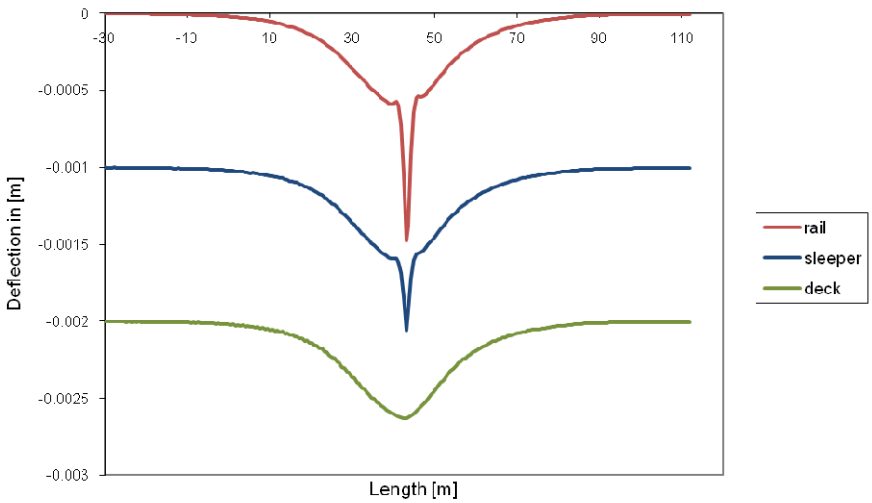

Figure 12: Deflection of the rail, sleeper and deck - one axle load.

Better analysis can be accomplished from the numerical results. Rail deflection is compared with deflections induced in sleepers and deck. The case of one load is represented in Figure 12, it is seen that the rail deflection is accentuated within a region of almost 3m, that encompasses 5 sleepers. This deflection peak propagates into sleepers but it is already slightly attenuated by railpads. More efficient attenuation is performed by the ballast layer, as expected. Deck deflection is therefore already smooth. The case of two opposing loads is shown in Figure 13. Rail deflection and other levels are related to the first load. Augmented displacements due to the second load are clearly visible. In Figure 14 torsional resistance is evaluated by comparison of deflections of longitudinal extremities of the upper deck.

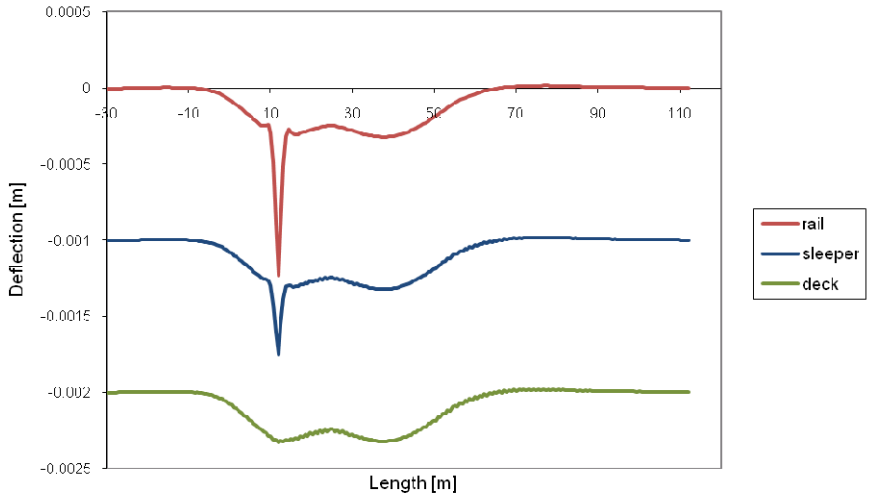

Figure 13: Deflection of the rail, sleeper and deck - two axle loads moving in opposing directions.

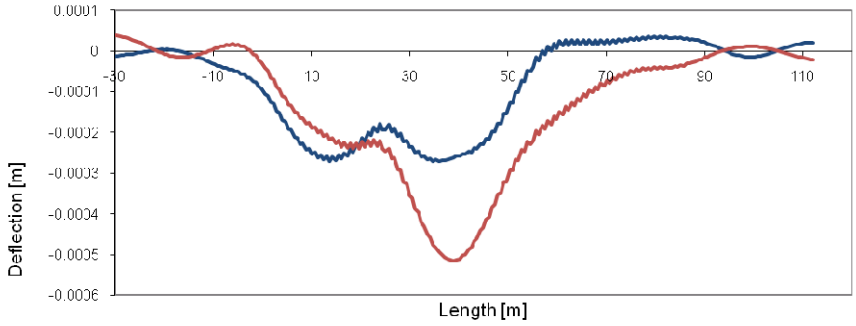

Figure 14: Deflection of the deck longitudinal extremity close to the first load (blue line) and to the second load (red line).

5 Parametric and statistical analyses

For the statistical analysis the predefined module ANOVA of Matlab software is used, that outputs the relevant data, namely:

- Histograms of the frequencies of the key results;
- Half normal plots with relevant key parameters pointed out;
- ANOVA table for the selected key results.

The selected key parameters and key results are presented in Table 5. For each of these parameters according to the experimental base the low and the high level must be selected. These are given in Table 6.

Key parameters	Key results
A. Ballast stiffness	Fundamental frequency
B. Train speed	Torsional frequency
C. Number of trains	Acceleration
	Rail deflection

Table 5: Key parameters and results.

Factor	Low level	High level
A	80% stiffness	100% stiffness
B	50 m/s	60 m/s
C	1	2

Table 6: High and low levels of key parameters.

For preliminary tests eight analyses were run on the first modulus and maximum displacement oriented downward was extracted.

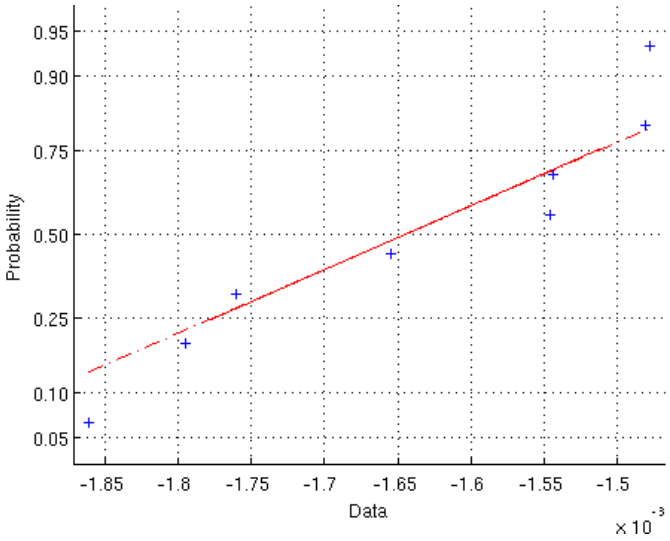

Figure 15: Normal probability plot.

These eight analyses were obtained by all combinations of low and high levels of factors defined in Table 6. Results obtained are summarized in Table 7 and Figure 15. It is clearly seen high dominance of the number of trains, as expected. Figure 15 shows probability versus residuals obtained.

Source	Sum Sq.	d.f	Mean Sq.	F	Prob>F
A	$1.07069 \cdot 10^{-9}$	1	$1.07069 \cdot 10^{-9}$	0.24	0.6515
B	$7.62674 \cdot 10^{-9}$	1	$7.62674 \cdot 10^{-9}$	1.69	0.2632
C	$1.31382 \cdot 10^{-7}$	1	$1.31382 \cdot 10^{-7}$	29.14	0.0057
Error	$1.80317 \cdot 10^{-8}$	4	$4.50793 \cdot 10^{-9}$		
Total	$1.58111 \cdot 10^{-7}$	7			

Table 7: ANOVA table for maximum deflection.

6 Conclusions

In this paper, factorial experimentation in simulating railway bridge dynamics was exemplified by screening the individual and joint effect of some key parameters. The statistical theory proved to be relevant and meaningful, easy to implement and yet very powerful.

Acknowledgements

The authors greatly appreciate support from Fundação para a Ciência e a Tecnologia of the Portuguese Ministry of Science and Technology, covering some expenses related to participation at RW2012 and supporting the execution of this work through the project grant PTDC/EME-PME/01419/2008: “SMARTRACK - SysteM dynamics Assessment of Railway TRACKs: a vehicle-infrastructure integrated approach”.

References

[1] ANSYS, Inc. Documentation for Release 12.1, Swanson Analysis Systems IP, Inc., November 2009.

[2] J. Lysmer, R.L. Kuhlemeyer, “Finite dynamic model for infinite media”, Journal of the Engineering Mechanics Division, ASCE, 95(EM4), 859-877, 1969.

[3] Z. Dimitrovová, A.F.S. Rodrigues, "An Enhanced Moving Window Method: Applications to High-Speed Tracks", in B.H.V. Topping, Y. Tsompanakis, (Editors), "Proceedings of the Thirteenth International Conference on Civil, Structural and Environmental Engineering Computing", Civil-Comp Press, Stirlingshire, UK, Paper 6, 2011. doi:10.4203/ccp.96.6

[4] T. Dahlberg, “Dynamic interaction between train and non-linear railway track model”, 4th International Conference on Structural Dynamics, EURODYN2002, H. Grundmann, G.I. Schueller (editors), Munich,

Germany, 2-5 September 2002, pp. 1155-1160.
[5] J.C.O. Nielsen, J. Oscarsson, “Simulation of dynamic train–track interaction with state-dependent track properties”, Journal of Sound and Vibration 275, 515–532, 2004.
[6] T. Mazilu, M. Dumitriu, "On the Steady State Interaction between an Asymmetric Wheelset and Track", in B.H.V. Topping, Y. Tsompanakis, (Editors), "Proceedings of the Thirteenth International Conference on Civil, Structural and Environmental Engineering Computing", Civil-Comp Press, Stirlingshire, UK, Paper 27, 2011. doi:10.4203/ccp.96.27
[7] E. Kausel, “Local transmitting boundaries”, Journal of Engineering Mechanics, 114, 1011-1027, 1988.